JOURNAL OF MATERIALS SCIENCE: MATERIALS IN MEDICINE 11 (2000) 569–578

Modeling of damage to articulating surfaces by third body particles in total joint replacements

C. M. McNIE, D. C. BARTON, J. FISHER*
School of Mechanical Engineering, University of Leeds, Leeds LS2 9JT, UK
E-mail: men6jf@leeds.ac.uk

M. H. STONE
Leeds General Infirmary, Leeds LS1 3EX, UK

Numerous small scratches and some larger scratches have been observed on metallic femoral heads of explanted hip prostheses, with the larger scratches believed to be a major contributor to increased wear of the polyethylene acetabular cups. Previous work in our group has shown that smaller scratches, with a mean lip height up to 0.35 μm, can be caused by bone cement and bone particles up to 500 μm in size [1]. However, the larger scratches were not readily replicated with these particles. Therefore in this study experimental and theoretical models have been developed to investigate the damage caused by harder metallic and ceramic particles. Small 10 μm diameter spherical metallic particles were also found to produce small fine scratches on the metallic counterface. However larger diameter spherical metal particles greater than 100 μm in diameter, which were embedded in polyethylene pins, caused severe sharp scratching of the metallic counterface with scratch lips greater than 0.5 μm. This level of damage, which was comparable to the severe damage found *in vivo*, was also simulated by a three body finite element model. Thus the larger metal particles led to the type of damage which was predicted to increase wear dramatically. This technique for simulating severe *in vivo* third body damage using spherical metal particles was found to be reproducible and reliable and will be used in the future in hip simulator testing to replicate third body damage and wear.

1. Introduction

Scratches found on the hard counterfaces of total joint replacements (usually stainless steel or cobalt chrome articulating against UHMWPE) are believed to contribute to the increased wear of the UHMWPE components. The geometry of the scratches can also affect the morphology of UHMWPE wear debris and consequently the incidence of osteolysis. Scratches that occur on metallic femoral heads *in vivo* have been postulated to be caused by third bodies such as particles of bone, cement and/or metal, which have often been found embedded in acetabular cups and in the periprosthetic tissues [1–3]. If the mechanism behind scratch generation is more fully understood, steps can be taken to reduce the generation of damaging third bodies. It has been widely reported that clinically relevant scratches on a femoral head range from less than 0.1 μm high to greater than 1 μm [2–4]. The effect of bone and cement debris has been well documented and has been shown to produce the smaller ''background'' scratches found on the femoral head in the range 0.15–0.35 μm high [1]. This was found to be true for a wide range of cement particle sizes (up to 500 μm) and it is believed to be the small radio-opaque additives in the cement (1–10 μm) that causes this finer scratching. This previous work with bone cement and bone particles did not replicate the larger scratches that are found on some explanted femoral heads and which are not attributed to surgical tool damage. Larger scratches have been previously simulated, *in vitro*, using a diamond stylus and the effect on the wear characteristics of UHMWPE studied [2, 5]. It was shown that the scratch lip area has a major influence on the wear volume while the scratch lip aspect ratio affected the wear debris morphology.

Metallic debris, ranging from 1 to 500 μm in size, can be generated at the stem/bone interface or the stem/bone cement interface by fretting wear due to small micromotions [6] or due to loss of surface coatings [7]. The particles released can migrate into the articulating region and we postulate that these metallic particles may be the source of the larger scratches on the femoral head. However, until now, the effect of metal debris acting as third body particles has not been investigated.

Therefore, the effect of a range of sizes of spherical metal third body particles on the counterface scratch geometry has been investigated by experimental

*Author to whom all correspondence should be addressed.

methods. In addition, a finite element surface contact model has been developed to include the presence of a third body at the contact site and the effect of particle size and material properties have been investigated.

2. Methods

2.1. Experimental methods

Third body damage was simulated using stainless steel spheres embedded on the surface of a cylindrical polymer wear pin (9.5 mm diameter with a conical end and a 3 mm wear face) which represented the acetabular cup. This was then slid against stainless steel plates (with a 56×25 mm polished surface and 15 mm thickness) which represented the femoral head. The stainless steel counterface was polished to a surface roughness finish of $R_a < 0.02\,\mu m$. Stainless steel spheres with a nominal mean diameter of either 10 μm (80% at 10 μm), $150 \pm 75\,\mu m$ (± 1 standard deviation) or $300 \pm 150\,\mu m$ (± 1 standard deviation) were used. Microtomed GUR 412 UHMWPE wear pins that had been soaked in distilled water for two weeks were then pressed onto the particles under a static load of 240 N. The resulting pin surfaces were characterized using 3D profilometry and micro-photography. The pin surfaces after the spheres had been embedded are shown in Fig. 1. Each pin and plate were placed in a single station of a pin-on-plate tribometer, shown schematically in Fig. 2, with the stainless steel plate immersed in a bath of 100% bovine serum. The pins, under a load of 240 N, were traversed 30 mm in each direction along the stainless steel plate for 5 complete cycles at 0.5 Hz to create the scratches. In addition to these 5 cycle tests, two more tests were carried out: a pin embedded with 300 μm particles was traversed for a single cycle and a pin embedded with 10 μm particles was run for 1000 cycles. These scratches were then characterized using 3D profilometry and compared with the *in vivo* generated scratches previously characterized on explanted femoral heads [2].

2.2. The third body finite element model and method

The 2D plane strain finite element model consisted of a four noded linear element mesh as shown in Fig. 3. The semi-infinite lower block is representative of the acetabular cup and its material properties were elastic-plastic as shown in Fig. 4, with an elastic modulus of 1.1 GPa, a yield stress of 11.23 MPa and a Poisson's ratio of 0.3 based on tests in compression at high strain rates ($0.48\,s^{-1}$) which is close to physiological rates. The upper block, with a flat contact surface, is representative of the hard femoral head. A cylindrical shape was then incorporated as a free third body into the model i.e. allowed to displace and rotate. The material properties for both the hard counterface and the particles are outlined in Table I. The model was analyzed using ABAQUS version 5.6 [8]. The counterface was firstly pressed into full contact with the UHMWPE and was then forced to slide seven times the particle diameter at a relative velocity of $22\,mm\,s^{-1}$, the average sliding speed of a Charnley stainless steel head *in vivo*. A nominal frictional co-efficient of 0.1 was specified between the contacting surfaces.

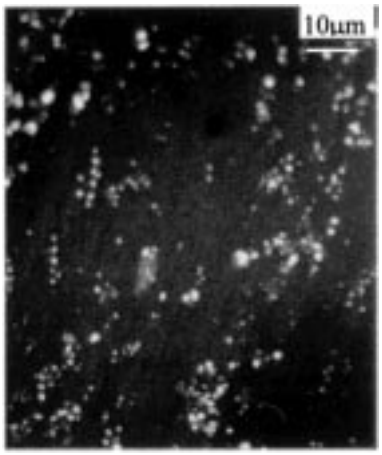

(a)

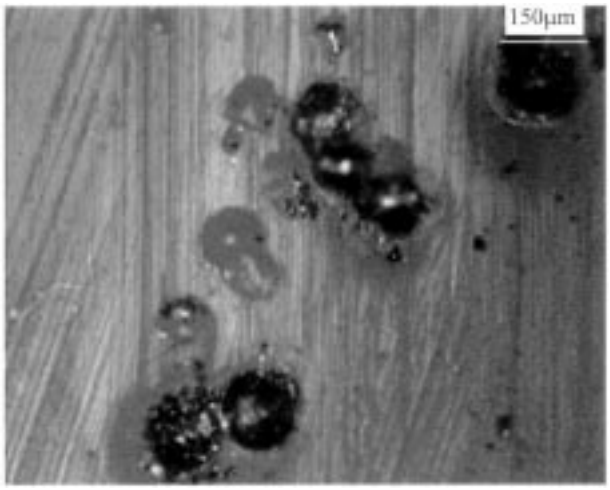

(b)

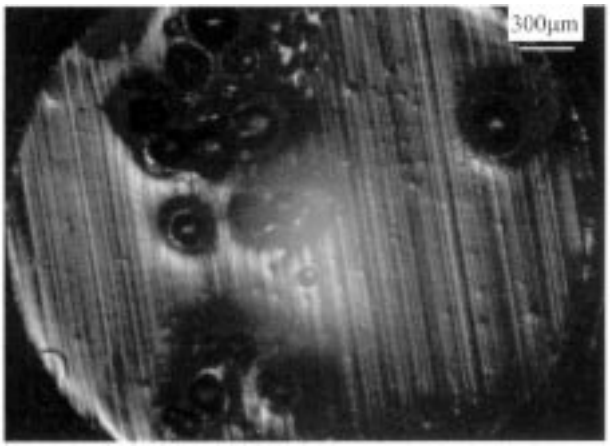

(c)

Figure 1 Photographs showing: (a) 10 μm; (b) 150 μm; (c) 300 μm particles embedded into pin surfaces.

Three material combinations were investigated with this model:

- the stainless steel particle diameter was varied (10, 150, 300 μm). The material properties of the stainless steel are outlined in Table I;
- a zirconia particle, 10 μm in size, was modeled with the material properties shown in Table I. The stainless steel counterface and the UHMWPE block remained the same;

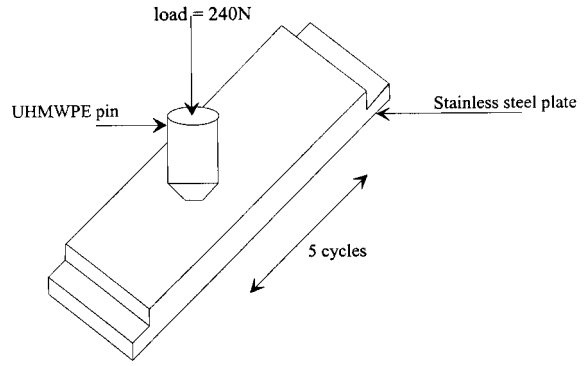

Figure 2 Schematic of the pin on plate scratch test.

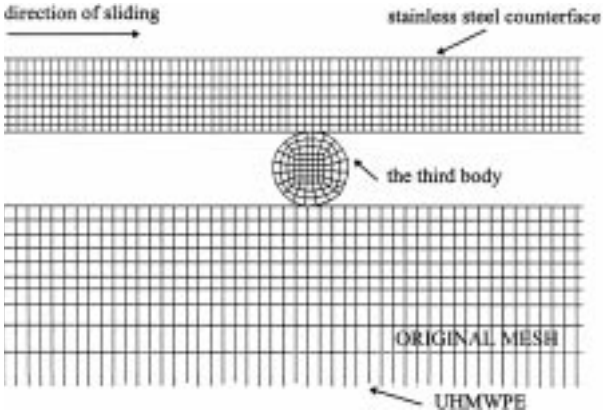

Figure 3 The finite element model with a third body.

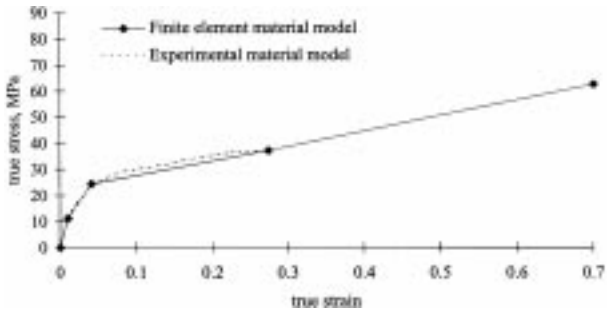

Figure 4 The stress-strain curve assumed for UHMWPE.

- a cobalt chrome particle, 300 μm in size, was modeled with the material properties shown in Table I. The counterface was now cobalt chrome whilst the UHMWPE block remained the same.

3. Experimental three body scratch test results

Fig. 5 shows the results of 3D profilometry of the scratches on plates that have had particle-embedded pins reciprocated over them for 5 cycles. It can be seen that the two large scratches (Fig. 5b and c) were made up of numerous smaller scratches within the larger scratch. The probable cause for this effect is clearly seen in Fig. 6, which shows a 300 μm particle after it has been slid over the plate surface for 5 cycles. The particle has a polished face containing many scratches which may have given rise to the many smaller scratches observed within each large scratch on the plate. Alternatively, it may have been due to small lateral movements of the particle with respect to the plate.

TABLE I Material properties used in the finite element model

Material property	Stainless steel	Cobalt chrome	Zirconia
E (GPa)	210	230	152
v	0.3	0.3	0.32
Yield stress (MPa)	200	220 or 500[a]	4000
Plastic tangent modulus (GPa)	1.08	7	0

[a] Two different yield stresses were used in the cobalt chrome material model to represent cast and forged material, respectively.

After 5 cycles, defined scratch paths had formed on all the plates. The mean scratch lip heights ranged from 0.1 μm for the 10 μm particles to approximately 2.3 μm for the 150 μm particles and 1.5 μm for the 300 μm particles, as shown in Fig. 7. Moreover, the mean scratch lip widths were found to increase with particle size, from 5 to 18 μm, with little difference between the 150 and 300 μm widths, Fig. 8. The scratch lips from a single pass of a pin embedded with a 300 μm particle were very similar to those from 5 cycles. In addition, the morphology of scratches that were generated from 1000 cycles using a pin embedded with 10 μm particles were similar to those from 5 cycles using 10 μm particles.

The scratch lip aspect ratio values followed the trend found with scratch lip height, Fig. 9; the mid-size particle (150 μm) was found to give the highest aspect ratio at 0.32. The aspect ratios of scratch lips that were generated from 1 cycle using a 300 μm particle were very close to those generated from 5 cycles. Similarly the aspect ratios of scratch lips from 10 μm particles sliding for 1000 cycles were slightly greater than those found from 5 cycles.

The plate surface that had been scratched by 10 μm particles for 1000 cycles is shown in Fig. 10. The plate surface was rough; the R_a had increased from 0.01 to 0.023 μm. The mean scratch lip height was 0.29 ± 0.074 μm (95% confidence limits) which was higher than the scratch lip heights found on the plates from 5 cycles with the 10 μm particles. A typical aspect ratio of a scratch lip was 0.09 ± 0.017 (95% confidence limits). Therefore, the scratch lips were found to be slightly larger and sharper from the 1000 cycle test compared with the 5 cycle test.

The 2D cross-sectional area of the scratch lip increased dramatically with particle size, as demonstrated by Fig. 11. The scratch lip cross-sectional areas generated from only half a cycle of a 300 μm particle were slightly higher compared with those for 5 cycles. Likewise, the scratch lip cross-sectional area of the scratches formed from 1000 cycles using 10 μm particles was similar in magnitude to that from 5 cycles of pins embedded with the same 10 μm particles. Fig. 12 shows that, as the particle size increased from 10 to 150 μm, the scratch valley depth increased. When the particle size was further increased from 150 to 300 μm, the valley depth was not significantly different. In addition, the number of cycles did not significantly affect the scratch valley depth.

When the pin with 10 μm particles embedded into its surface was cyclically slid over a plate 5 times, the majority of particles were left in the contact. However there were visible tracks left by the particles leaving the contact, as demonstrated in Fig. 13a. When the pin was

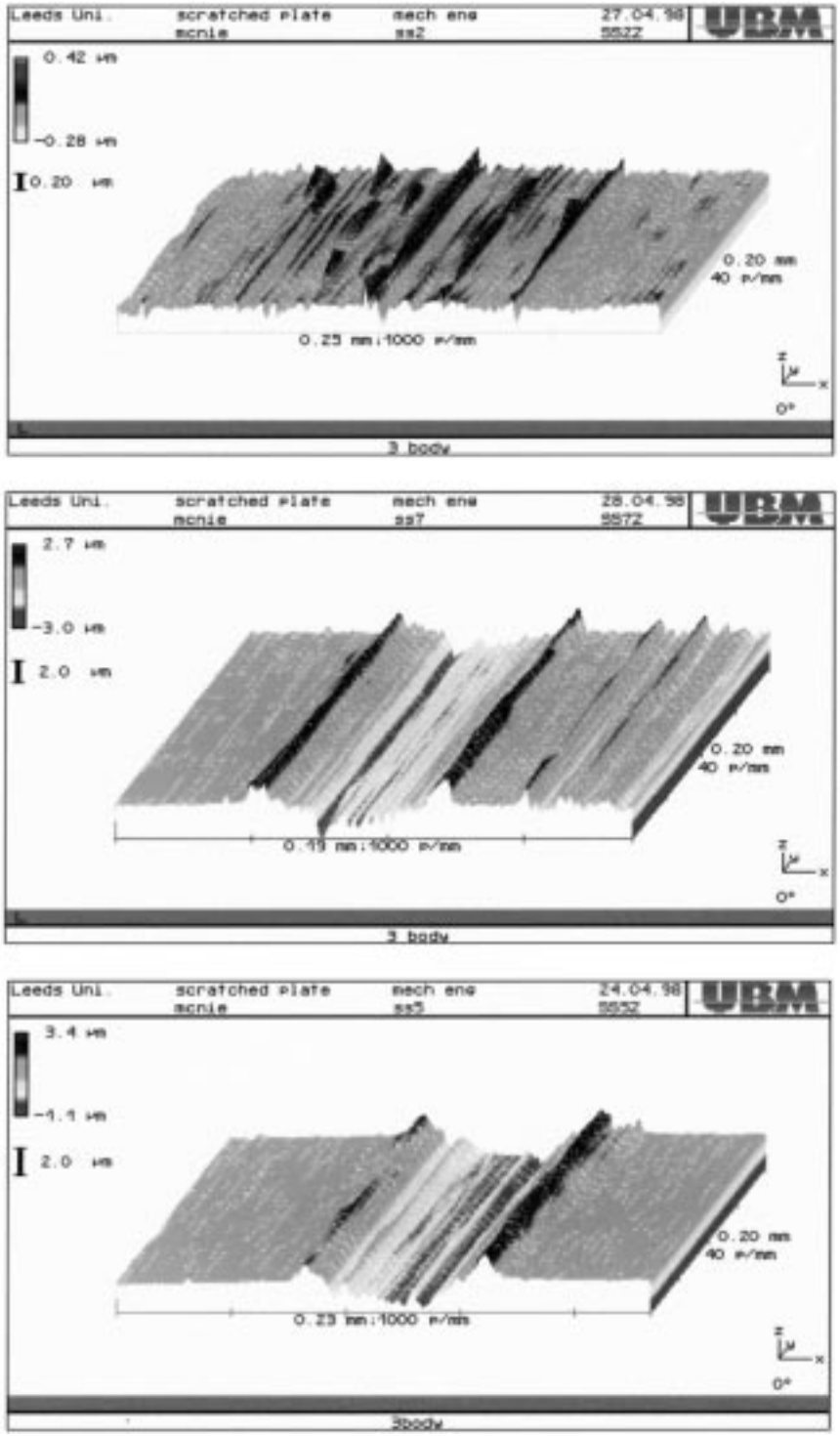

Figure 5 3D profiles of scratches on plates caused by: (a) 10 µm; (b) 150 µm; (c) 300 µm particles.

slid for 1000 cycles over the plate surface, it was observed that most of the particles had been removed from the contact, as demonstrated in Fig. 13b.

The surface profile of the scratch, after a single cycle of 300 µm particles over the plate surface, is shown in Fig. 14. The single prominent scratch lip was found to be similar in geometry to that found after 5 cycles. This uneven geometry of the scratch lip from a single cycle may possibly have been caused by the force on the pin face not being quite perpendicular to the plate. In addition, defined scratch tracks were seen on the pin surface embedded with larger particles (300 µm) where the particle had been drawn out of the contact. It is assumed that the particles embedded in the polymer loosened as a result of alternating friction forces due to the reciprocating motion of the pin. The particles were then able to move through the contact leaving these tracks in the polymer surface which are the result of plastic deformation of the surface.

4. Three body finite element model results

4.1. Effect of stainless steel particle size variation

The cylindrical third body in the finite element model, representative of a stainless steel particle, was varied in

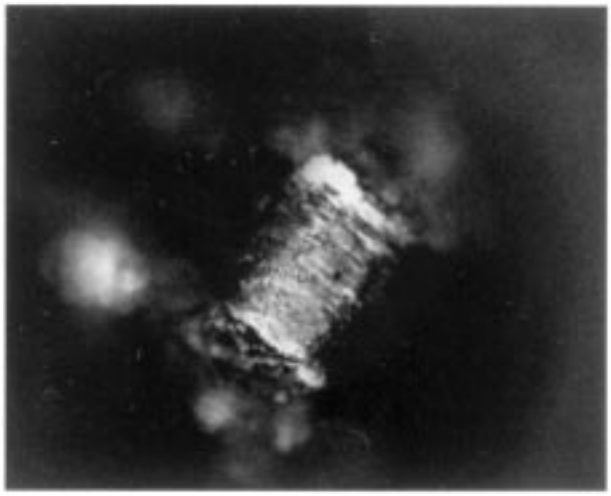

Figure 6 The polished face of a 300 μm particle.

size. Fig. 15 shows that the force required to fully indent the particles into the UHMWPE increased with particle size as expected. The actual number of 10, 150 and 300 μm particles on the pins was approximately 1300, 9 and 3, respectively. The force exerted by the UHMWPE pin in the scratch tests was 240 N, and therefore the 150 and 300 μm particles in the scratch tests may be assumed to have been fully indented while the 10 μm particles may have been only partially indented since, relatively, there were so many of them.

Since more force was required to push a larger particle into the UHMWPE, greater plastic indentation of the stainless steel surface occurred, as shown in Fig. 16. It should be noted that, to either side of this maximum indentation, small lips were observed (0.5 μm high for the 300 μm particle finite element model). Outward of these lips there was secondary minor deformation. This form of plastic disruption of the stainless steel surface was also observed in the experimental scratching of plates with particles, as shown particularly well in Fig. 17.

As a result of the increased loads applied, the maximum plastic strain increased with particle size in all sections of the model (the particle, the stainless steel counterface and the UHMWPE) as shown in Fig. 18. A typical plastic strain distribution in the FE model is shown in Fig. 19 for a 10 μm particle. The areas of the plastic strains in both the stainless steel counterface and the UHMWPE were found to be directly proportional to particle size. The particle was found to be most highly strained at the contact interface with the stainless steel counterface as expected. The particle was also found to rotate by 23° during the relative sliding. In addition, the particle was displaced horizontally by 0.5, 2.3, 5 μm for particle sizes of 10, 150, 300 μm, respectively. Thus it is predicted that, after many cycles, the particle may be able to move out of the contact and would undoubtedly leave a wear track/scar in the UHMWPE.

4.2. Effect of particle material variation

The results from the finite element model for a 10 μm stainless steel and zirconia particles are shown in

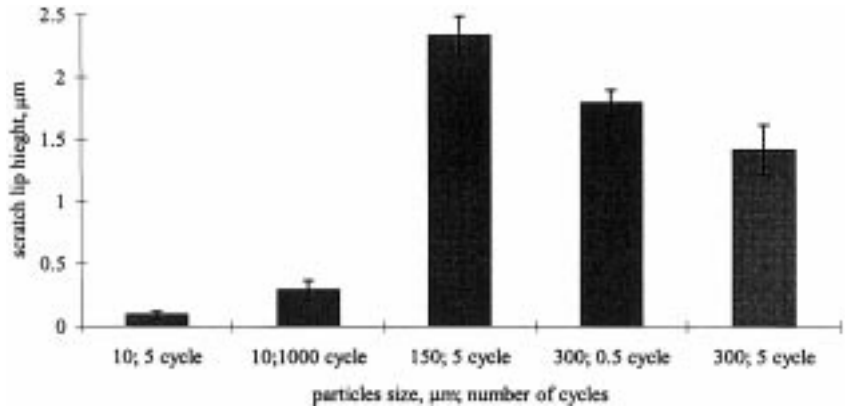

Figure 7 Variation of scratch lip height with particle size.

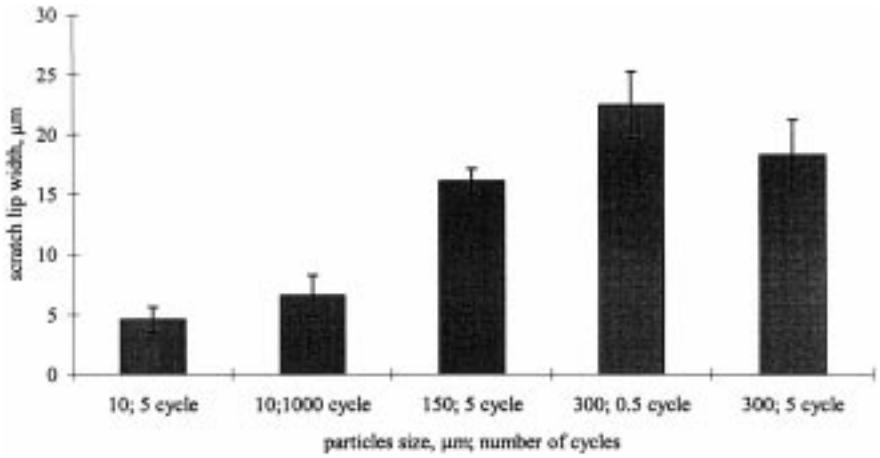

Figure 8 Variation of scratch lip width with particle size.

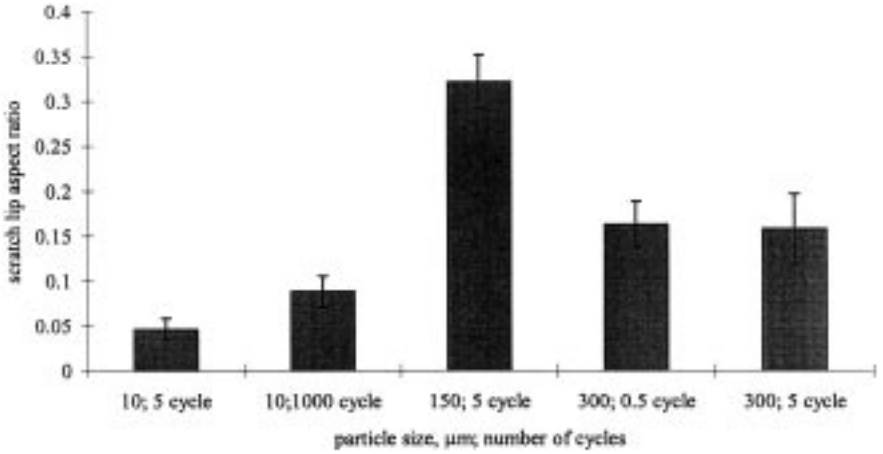

Figure 9 Variation of scratch lip aspect ratio with particle size.

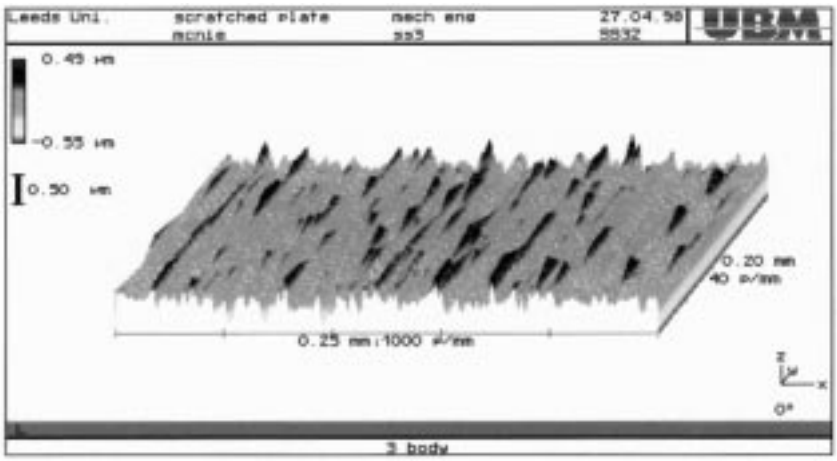

Figure 10 The plate surface after 1000 cycles of 10 µm particles.

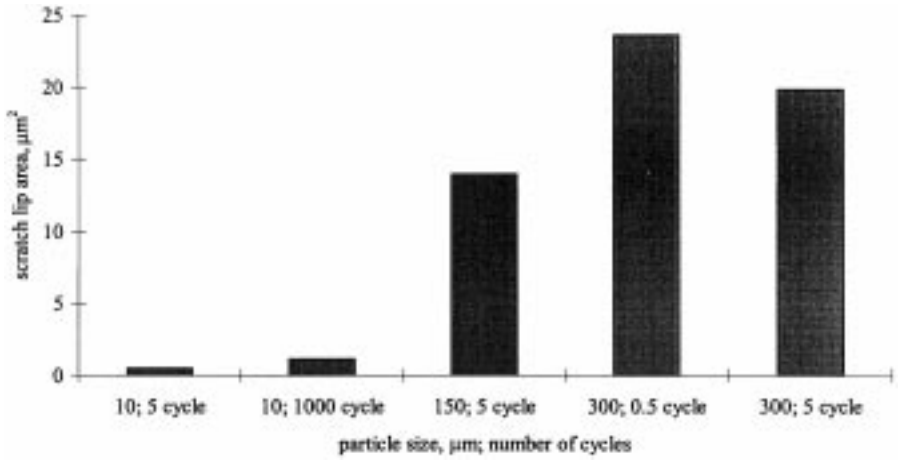

Figure 11 Variation of the 2D cross-sectional area of the scratch lip with particle size.

Table II. The same normal loads of 0.5 N were applied to the particles. Greater maxima of plastic strain occurred in the stainless steel counterface and the UHMWPE when the particle was zirconia because the harder zirconia particle did not deform plastically. In addition, the zirconia particle did not move as much in the contact as the stainless steel particle.

The results of like metallic particles and counterfaces sliding with respect to each other are shown in Table III for a cobalt chrome particle/counterface of yield stress 220 MPa (cast material). Similar plastic strains were found in the UHMWPE but vastly different plastic strains were observed in the metallic counterface due to the differences in material properties. The surface plastic indentations were found to be in close agreement for the two counterfaces (stainless steel and cast cobalt chrome), despite the differences in material properties. When the yield stress of the cobalt chrome was raised from 220 to 500 MPa, there was no plastic strain predicted in the spherical cobalt chrome particle or counterface.

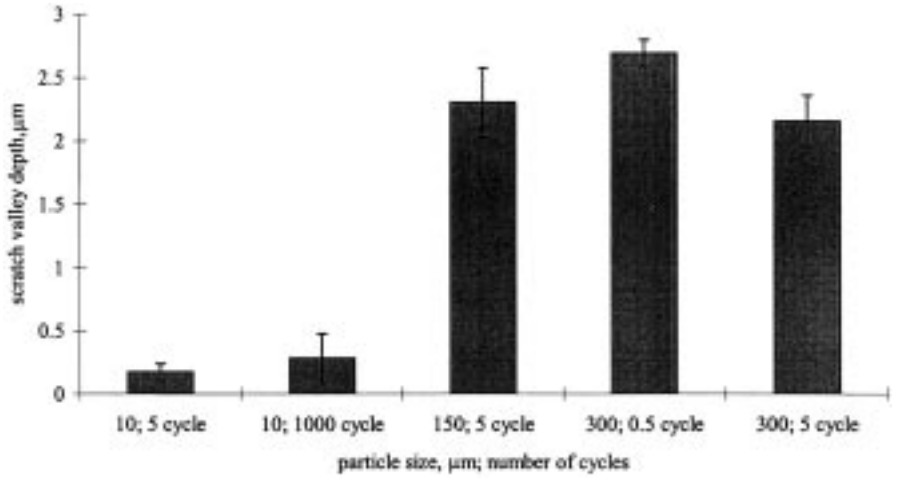

Figure 12 Variation of scratch valley depth with particle size.

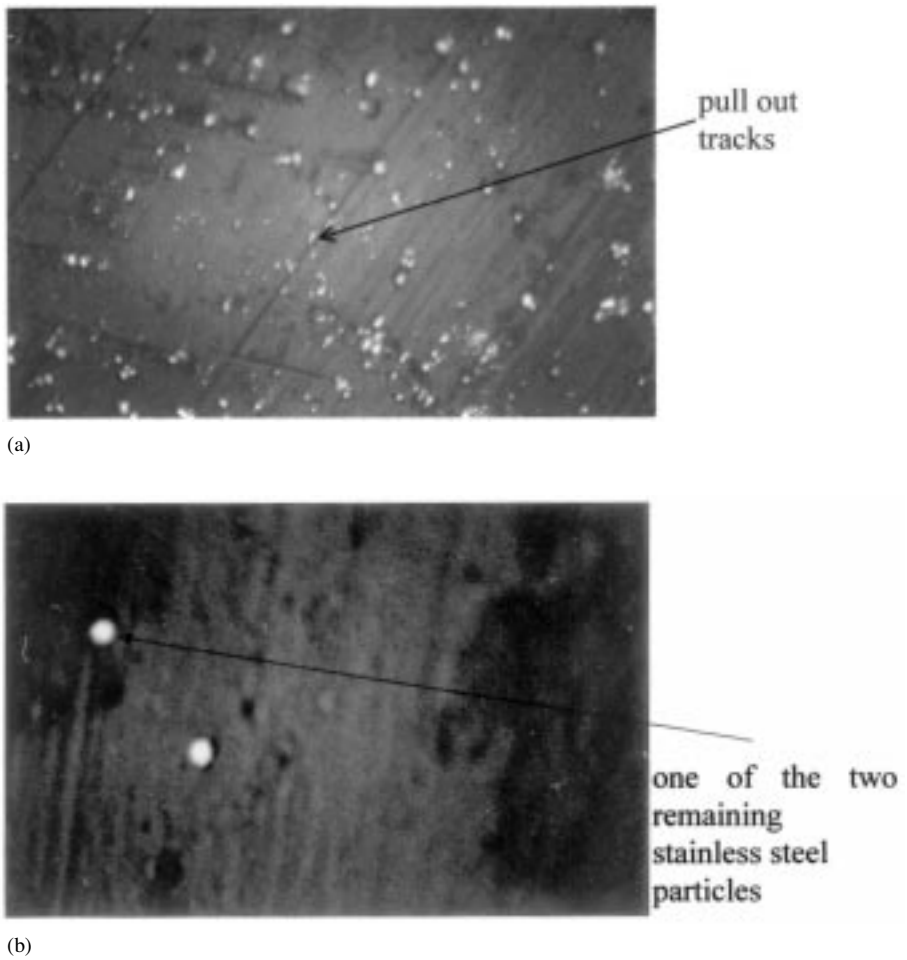

Figure 13 The pin surface embedded with 10 μm particles after (a) 5 cycles (magnification × 200) and (b) 1000 cycles (magnification × 400).

5. Discussion

Damaging metal debris can come from many sources: fretting wear of the stem at the bone/cement interface; the wear at the taper of a modular head; fixation screws and/or porous coatings. A wide range of particles sizes may be produced which can migrate into the contact area, consequently affecting the surface roughness of the femoral head and the wear of the acetabular cup. It has been shown experimentally in this paper that metallic particles can reproduce a range of scratches comparable to those found *in vivo*. The metal particles used in this study gave a wide range of scratch geometry, from the small scratch lips similar to those reported to have been caused by bone and cement particles [1] to the larger scratch lips that had not previously been replicated by third body particles *in vitro*. It has also been shown that only 5 cycles of the particles over the stainless steel counterface were adequate for producing deep scratches, and that the scratch lip geometry did not change significantly for less (0.5 cycles) or much greater (1000 cycles) duration of sliding. Therefore, all future

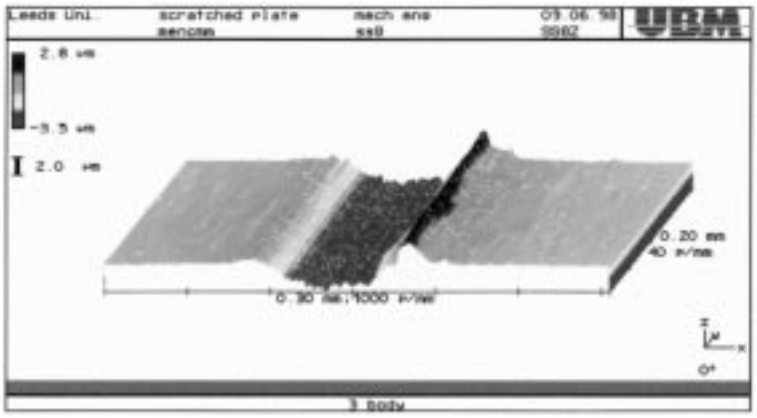

Figure 14 The plate surface after 1 cycle of 300 μm particles.

comments on the experimental scratch results will be based on results from the 5 cycle tests.

The range of scratch lip aspect ratios obtained from this method of creating scratches were found to relate closely to those measured *in vivo* [4], Table IV. Furthermore it can be seen from Table IV that the scratches formed by the diamond stylus technique tended to be sharper than the scratches observed on explanted femoral heads or produced by the abrasive action of the particles. Also the particle generated scratch lip heights and widths were closer in magnitude and range to those found *in vivo* than those formed by the diamond stylus. Therefore, the technique of using particles to generate scratches is considered superior to the diamond stylus method as the scratches produced tended to be more representative of those found *in vivo* and therefore also of those modeled in the asperity based finite element model reported in [4].

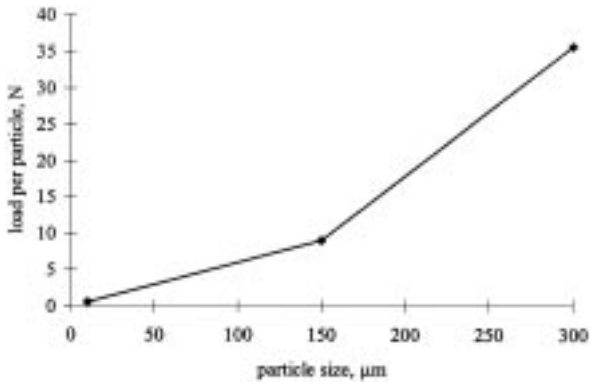

Figure 15 Variation of the load required to fully indent the particle as a function of particle size.

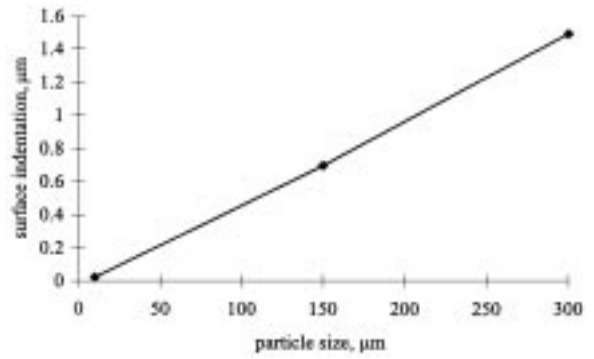

Figure 16 Variation of the plastic indentation of the stainless steel counterface with particle size.

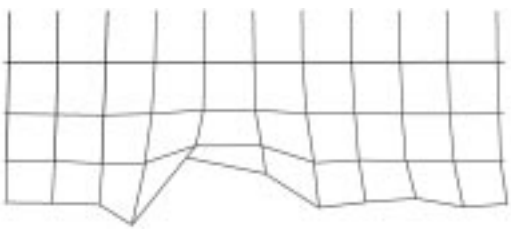

Figure 17 The stainless steel counterface after full contact with a 10 μm particle (magnification × 50).

It has been predicted that the larger scratch lips generated by larger particles (150 and 300 μm) will lead to a greater volume of UHMWPE wear debris per scratch [4]. In addition, the aspect ratio of the scratch lips was larger for 150 and 300 μm particles. Again, an increased scratch lip aspect ratio has been found in previous wear tests to increase the proportion of micron size UHMWPE wear debris [4]. Therefore, it is postulated that these large scratch lips of high aspect ratio, generated from the larger particles, will produce not only a greater volume of UHMWPE wear particles but also a greater proportion of sub-micron sized particles. These two factors together would lead to a greater likelihood of osteolysis.

There was a large difference in scratch geometry when the particle size was increased from 10 to 150 μm in diameter. However, when the particle size increased from 150 to 300 μm, the effect reduced noticeably. Another separate study [9] has shown that the wear rate (and groove geometry) of a steel counterface increased with the size of the abrading particle size but above a critical size, around 120 μm in diameter, the effect on

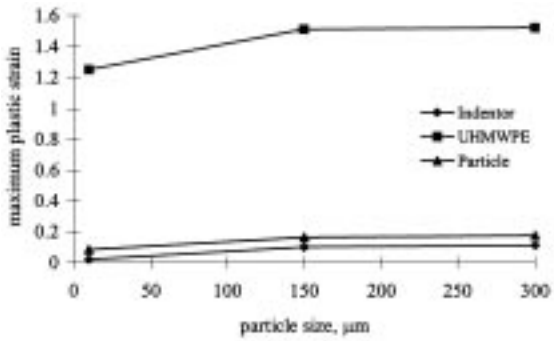

Figure 18 Variation of maximum plastic strains in the three bodies of the FE model with particle size.

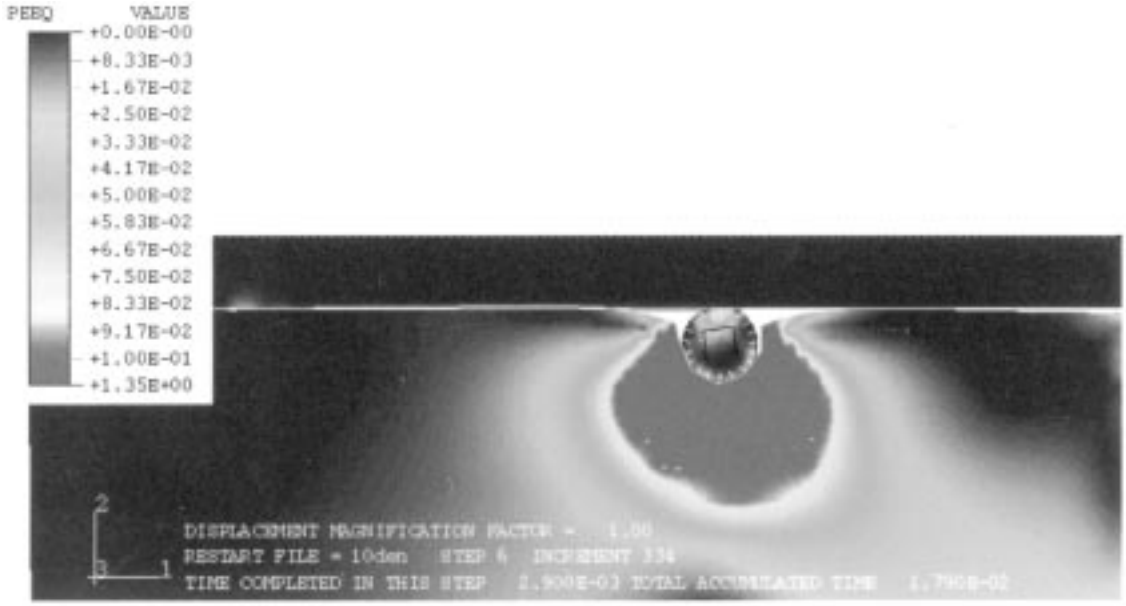

Figure 19 Contours of strain in the three body finite element model.

wear rate was reduced. In addition, this effect of particle size on wear rate reduced when the tip radius of the particle tended to zero, regardless of the load, because full plastic indentation was always obtained and the groove geometry generated remained constant. This correlates with the fact the scratch geometry increased dramatically when 150 μm particles were used instead of 10 μm particles and not when 300 μm particles were used instead of 150 μm particles.

TABLE II Comparison of finite element model results for stainless steel and zirconia particles

Measurement	Stainless steel particle (10 μm)	Zirconia particle (10 μm)
Plastic strain in indentor	0.02	0.10
Plastic strain in UHMWPE	1.25	1.65
Plastic strain in particle	0.08	0
Indentor surface deformation (μm)	0.02	0.08
Horizontal movement of particle (μm)	4.1	1.50

TABLE III Comparison of finite element results for stainless steel and cobalt chrome 300 μm particles

Measurement	Stainless steel indentor and particle (300 μm)	CoCr indentor and particle (300 μm)
Plastic strain in indentor	0.11	0.0324
Plastic strain in UHMWPE	1.52	1.4
Plastic strain in particle	0.17	0.0561
Indentor deformation (μm)	2.3	2.3
Horizontal movement of particle (μm)	1.5	3.3

TABLE IV Comparison of scratch lip geometry created using different methods

Scratch method	Lip height (μm)	Lip width (μm)	Lip aspect ratio
In vivo	0.1–10	5–100	0.01–0.45
Diamond stylus	0.8–1.8	3–8.2	0.29–0.8
Particles	0.1–2.5	2–20	0.05–0.3

It should be noted that the particles used in these tests were all spherical. However, many different particle morphologies occur *in vivo* e.g. particles with jagged edges. If the particle was, for example, conical in shape and protruding out of the UHMWPE, the aspect ratio would be much greater compared with a spherical particle of the same nominal size. This would mean that deeper and narrower scratches would be likely to be produced, with the scratch lips most probably having higher aspect ratios, resulting in smaller wear debris with greater osteolytic potential. Moreover smaller irregular shaped particles are likely to produce greater scratch lip height than spherical particles.

When particles around 300 μm in size were slid over like-metal heads, severe scratching occurred as shown in the experimental tests and also as predicted by the finite element models (stainless steel being scratched by a stainless steel particle and cobalt chrome being scratched by a cobalt chrome particle). The most likely source for these large metal particles are from porous metal coatings which consist of sintered beads, around 300 μm in diameter, and are most commonly used in cementless prosthesis. Therefore, cementless total hip replacements may be more susceptible to the severe scratching that can lead to a higher number of micron size UHMWPE wear particles and hence a higher potential for osteolysis. This is supported by an explant study of cobalt chrome femoral heads [7], which found that scratched areas were more common on femoral heads from cementless total hip replacements compared with those from cemented systems. In addition, lysis was found to be a more common mode of failure for cementless systems.

The majority of stems and cup backings from the cementless systems in this study [7] were porous-coated with cobalt chrome beads. Furthermore this series of explants are likely to have been made from cast cobalt chrome which is known to have a lower yield stress than forged cobalt chrome which is the current industry standard. The finite element models have shown that the yield stress is critical in determining the amount of

plastic deformation in the metallic counterface. Thus, these older explants are likely to be more susceptible to scratching than current forged cobalt chrome heads.

It was shown in [7] that it was not only bone and cement particles that were responsible for scratching but also metallic particles. Indeed it can be concluded that the cement debris (consisting of 10 μm zirconia particles) from cemented stems had a less damaging effect on the femoral head surface as smaller, less sharp scratches were produced compared with the scratches produced by large metal particles from porous coatings.

The present three body finite element model predicted that the maximum plastic strains in the UHMWPE also increase with increasing particle size. This means that the UHMWPE is more likely to produce wear debris from a reduced number of cycles for large particles because of the increased residual strains. In addition, the finite element model predicted the order of severity of the scratch depths (counterface surface indentation) from different particle sizes. However, to enable a full study of particle motion and to predict in more detail the scratch lip geometry, the finite element model needs to be developed in 3-dimensions.

It has been observed frequently in these scratch tests and other laboratory experiments [2] that the third body tends to migrate from the contact site. The FE model showed how the particle can move out of the contact after many cycles as significant translation of the particle was predicted to occur after only one cycle. In addition, the predicted translation and rotation of the particle may explain why scratch lips, both *in vivo* and *in vitro*, tended to be non-symmetrical and non-uniform with respect to the axis of the scratch.

Deeper scratches were predicted to occur by the FE model in the stainless steel counterface when the material of the 10 μm particle was zirconia which is a harder material. Less translation of the particle was also predicted when the particle was modeled as zirconia. Therefore, the particle would take longer to move out of the contact and there would be more opportunity for scratches to occur. These two observations confirm the findings of a previous study of the morphology of scratches due to the presence of zirconia particles around 10 μm in size which showed that the scratches occurred frequently and were sub-micron in size [1].

150 and 300 μm stainless steel particles embedded in the polyethylene generated typical *in vivo* scratches seen on explanted femoral heads. This new technique of simulating severe *in vivo* third body damage using spherical particles is an easily reproducible method. This method can be used to precisely scratch femoral heads and hence could become part of a standard hip simulator test protocol which would test for the ability of a femoral head material to resist scratching and also for the resistance of the soft counterface to any scratch lips that are formed.

Given that the mechanism of scratch damage is now understood in greater detail, steps may be taken towards developing an improved design. For example, porous coatings are made from the most damaging particle type (300 μm) and therefore should be modified.

6. Conclusions

- Spherical stainless steel particles embedded in the UHMWPE replicate typical *in vivo* damage observed on the counterface of explanted femoral heads.
- 10 μm particles replicate the numerous sub-micron scratches.
- 150 and 300 μm particles replicate the larger scratches which occur less frequently.
- A three body finite element model can be used to predict the nature and severity of the scratch damage.
- The particle scratching method could become part of standard hip simulator test protocols, so that the worst conditions occurring *in vivo* can be simulated on a routine basis.

Acknowledgments

This work has been supported by the Wellcome Trust, and the DTI CAM1 Project on accelerated test methods to predict the durability of materials and surface treatment employed for artificial hip joints.

References

1. H. MINAKAWA, M. STONE, B. M. WROBLEWSKI, M. PORTER, E. INGHAM and J. FISHER, in ''44th Annual Meeting of the ORS'', (1998) p. 779.
2. L. CARAVIA, D. DOWSON, F. FISHER and B. JOBBINS, *J. of Engineering in Medicine* **204H** (1990) 65.
3. G. H. ISSAC, J. R. ATKINSON, D. DOWSON, P. D. KENNEDY and M. R. SMITH, *Eng. Med.* **16(3)** (1987) 167.
4. C. M. MCNIE, D. C. BARTON, E. INGHAM, M. H. STONE, J. L. TIPPER and J. FISHER, *J. Mat. Sci.: Mat. Med.*, in press (1998).
5. J. FISHER, P. FIRKINS, E. A. REEVES, J. L. HAILEY and G. H. ISSAC, *J. of Eng. in Medicine*. **209H** (1995) 263.
6. D. L. SHARDLOW, T. GREEN, J. B. MATTHEWS, M. WROBLEWSKI, M. H. STONE and J. FISHER, ''8th Annual conference of EORS'' (1998) p. 062.
7. M. JASTY, C. BRAGDON, K. LEE, A. HANSON and W. HARRIS, *J.B.J.S.* **76-B(1)** (1994) 73.
8. HIBBET, KARLSSON, SORENSEN, INC., ABAQUS, Standard/ User's Manual, Version 5.6, (1996).
9. J. JIANG, F. SHENG and F. REN, *Wear* **217** (1998) 35.

Received 6 October 1998
and accepted 29 April 1999